Full Paper

4,6-Diaryl/heteroarylpyrimidin-2(1*H*)-ones as a New Class of Xanthine Oxidase Inhibitors

Shiwani Shukla[1], Dinesh Kumar[1], Ritu Ojha[1], Manish K. Gupta[2], Kunal Nepali[1], and Preet M. S. Bedi[1]

[1] Department of Pharmaceutical Sciences, Guru Nanak Dev University, Amritsar, Punjab, India
[2] Department of Pharmaceutical Chemistry, ISF College of Pharmacy, Moga, Punjab, India

A series of 4,6-diaryl/heteroarylpyrimidones was synthesized employing silica-supported fluoroboric acid under solvent-free conditions in a microwave reactor. The catalytic influence of HBF_4-SiO_2 was investigated in detail to optimize the reaction conditions. The synthesized compounds were evaluated for *in vitro* xanthine oxidase (XO) inhibitory activity for the first time. Structure-activity relationship analyses are also presented. Among the synthesized compounds, VA-5, -9, -10, -12, -22, -23, and -25 were the active inhibitors with IC_{50} values ranging from 6.45 to 13.46 μM. Compound VA-25 with a pyridinyl ring as ring A and a thiophenyl ring as ring B emerged as the most potent XO inhibitor ($IC_{50} = 6.45$ μM) in comparison to allopurinol ($IC_{50} = 12.24$ μM). Some of the important interactions of VA-25 with the amino acid residues of the active site of XO were figured out by molecular modeling studies.

Keywords: Catalyst / Fluoroboric acid / Inhibitors / Microwave radiation / Pyrimidones / Silica / Xanthine oxidase

Received: January 27, 2014; Revised: February 27, 2014; Accepted: March 12, 2014

DOI 10.1002/ardp.201400031

Introduction

Xanthine oxidase (XO), a versatile molybdoflavoprotein that catalyzes oxidative hydroxylation of purine substrates to produce uric acid and subsequent reduction of oxygen at the flavin center with the generation of reactive oxygen species (ROS), either as superoxide anion radical or hydrogen [1–3] peroxide, leads to many diseases such as gout and at least symptoms of diseases such as oxidative damage to the tissue [2]. Involvement of reactive oxygen species in pathological events including inflammation, metabolic disorders, cellular ageing, atherosclerosis, and carcinogenesis is well reported. Increased XO serum level in pathological states such as hepatitis, inflammation, cancer, etc. indicates that XO inhibitor may result in broad-spectrum therapeutics for gout, cancer, inflammation, and oxidative damage [4]. Despite the potential of allopurinol [3, 5], 2-alkyl hypoxanthines [6], pterin, and 6-formylpterin [7] as XO inhibitors, their use associated with Steven Johnson syndrome and worsening of renal function induced in some of the patients [2–4] has led to the continuous search for novel scaffolds as XO inhibitors.

We have been actively involved in the design, synthesis, and evaluation of XO inhibitors during the recent past [4, 8–10]. Recently our research group explored the XO inhibitory potential of a series of *N*-acetyl pyrazolines [8] and *N*-(1,3-diaryl-3-oxopropyl)amides [9] (Fig. 1). The structure–activity relationship established on the basis of *in vitro* evaluation and the molecular modeling studies of both the classes revealed some important structural features required for inhibiting the enzyme such as (i) aryl/heteroaryl rings linked via a 3-carbon open chain or a cyclic linker with heteroatoms on 1- and 3-carbon, (ii) sites for hydrophobic interaction, arene–arene interaction, electrostatic interactions (Fig. 1) and (iii) appropriately placed carbonyl functionality for hydrogen bonding interactions (Fig. 1). The results also indicated that the dependence of inhibitory potential on the electronic and steric effects varies with the nature of the linker (a cyclic linker as in case of *N*-acetyl pyrazolines or a open chain linker as in case of *N*-(1,3-diaryl-3-oxopropyl)amides. With this background, the present study explores the potential of a series of 4,6-diarylpyrimidin-2(1*H*)-ones (target compounds, Fig. 1) as a new class of XO inhibitors. The target compounds employ pyrimidone ring as the linker for the two aryl rings that allows similar arrangement of the two aryl

Correspondence: Dr. Kunal Nepali, Department of Pharmaceutical Sciences, Guru Nanak Dev Univeristy, Amritsar, Punjab-143005, India
E-mail: kunal_8855@rediffmail.com, kunalbvk3@gmail.com
Fax: +91-1832258819

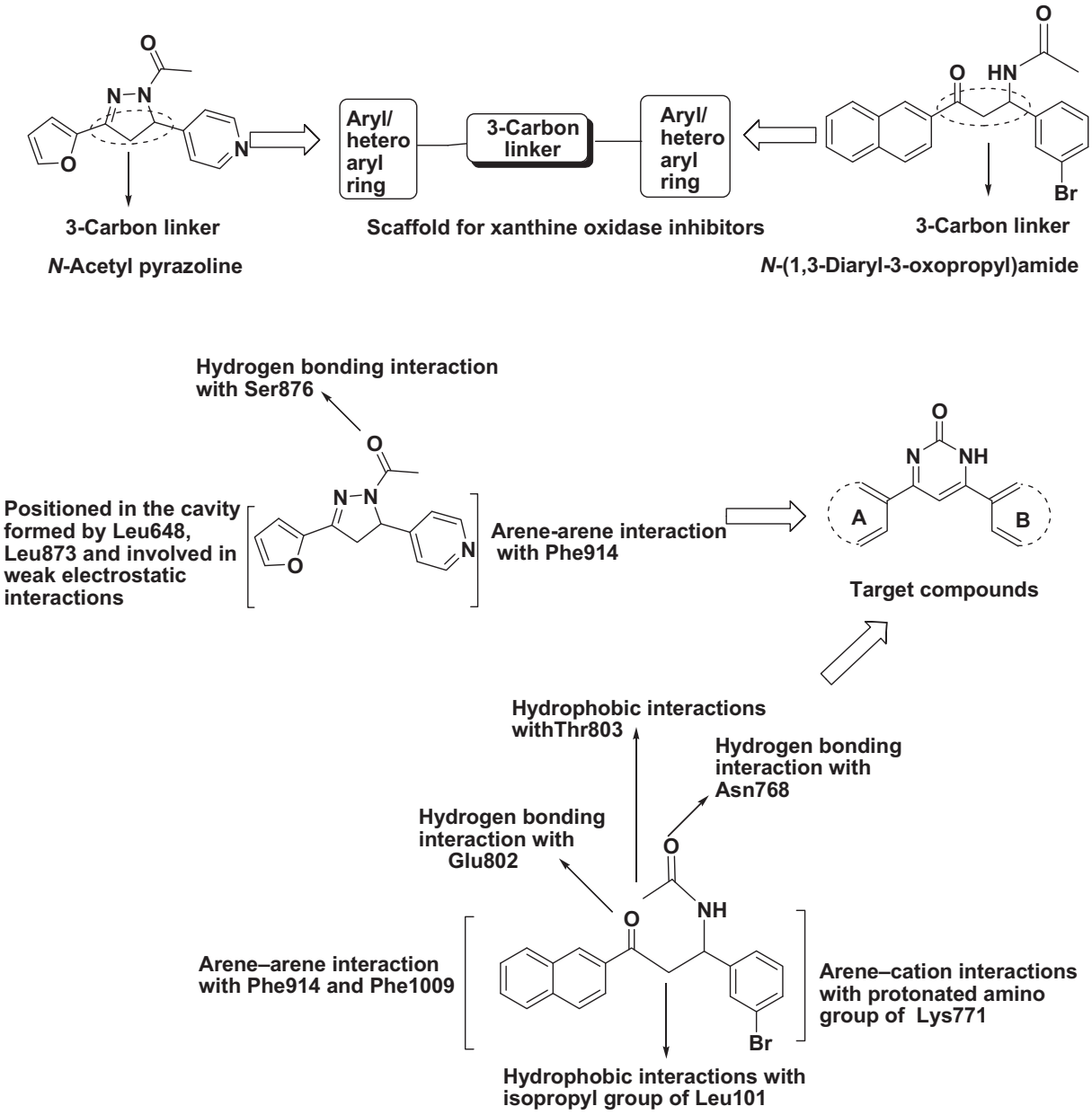

Figure 1. Structural features and interactions for XO inhibition.

rings as in case of the earlier reported inhibitors by us [8, 9] (Fig. 1).

As a part of our continued search for efficient methodologies for XO inhibitors [10], a series of 4,6-diaryl/heteroaryl pyrimidones as a new class of XO inhibitors was designed and synthesized via silica-supported fluoroboric acid under neat conditions in a microwave reactor. Though the Biginelli reaction has been well explored for the synthesis of 3,4-dihydropyrimidinones [11], three-component cyclocondensation of an aldehyde, acetophenone, and urea resulting in the formation of 4,6-diarylpyrimidin-2(1*H*)-ones (Fig. 1) still requires an efficient protocol. The existing methodologies for the synthesis of 4,6-diarylpyrimidin-2(1*H*)-ones lack in one or more of the following – two-step synthesis [12a],

applicabilty to limited substrates (not investigated for heteroaryl ketones/aldehydes and bicyclic ketones/aldehydes) [12b, 12c], and use of hazardous solvents [12d]. This tempted us to investigate the reaction under microwave conditions employing a silicated fluoroboric acid and a variety of substrates such as (i) aryl/heteroaryl ketones, (ii) aryl/heteroaryl aldehydes, (iii) bicyclic ketones, (iv) bicyclic aldehydes and (v) aldehydes and ketones with electronically diverse substituents. The use of catalysts immobilized on solid supports has received considerable attention [13] as adsorption of reagent onto an insoluble inorganic or organic support improves activity and selectivity of reagent by increasing effective surface area of reagent dispersed on a support up to 100 times and also helps in preventing the release of reaction residues into the environment for achieving environment-friendly organic synthesis [14]. Moreover multicomponent synthesis by Lewis acids/Bronsted acids have gained enough attention in the recent past [15]. Fluoroboric acid was employed in the present study as it is a weak protic acid that when adsorbed on silica would circumvent problem of side reaction for acid-sensitive substrate [13c].

Results

Chemistry

In an attempt to investigate the catalytic efficiency of fluoroboric acid adsorbed on silica, a model reaction (Scheme 1) was performed exposing a mixture of aromatic aldehyde (5.0 mmol, 1 eq), aromatic ketone (5.0 mmol, 1 eq), urea (5.0 mmol, 1 eq), and varying mol% of silicated fluoroboric acids to microwave radiations (varying time) in a microwave synthesizer operating at 150°C with the maximum microwave power of 400 W for the synthesis of target compound (Table 1).

In order to examine the substrate scope of this reaction, various aromatic ketones/aldehydes were used (Tables 1 and 2), and from the results, we could see that all reactions with aromatic aldehydes/ketones possesing electronically diverse substituents as well as heteroaryl aldehydes/ketones proceeded smoothly to afford the corresponding pyrimidones in good to excellents yields. Careful observation of Table 1 indicates a decrease in percentage yield of the target compounds on increasing the time of exposure of microwave irradiation from 10 to 15 min and further to 20 min. The optimum reaction conditions involve the use of 5 mol% of the catalyst for 10 min in a microwave reactor. The percentage yield of the pyrimidones was generally high ranging from 62 to 94%. In general pyrimidones with halogen-substituted phenyl rings (at both 4 and 6 positions) were obtained in excellent percentage yield (>90%). The excellent yields with halogens-substituted phenyl rings could be attributed to the dominant −I effect of halogens in comparison to +R effect. Pyrimidones with phenyl ring possessing OCH_3 groups were also obtained in good yield (80–90%). However, the yields were slightly less in comparison to pyrimidones with halogen-substituted phenyl groups. This might be due to dominant +R effect of methoxy groups in comparison to −I effect. Pyrimidones with heteroaryl rings and bicyclic rings were obtained in moderate yields (62–71%), indicating the versatility of the supported catalyst towards electronically and sterically diverse substitutents. Applicability to a variety of substrates (bicyclic/aromatic/heteroaromatic ketones and aldehydes), short reaction time, high yields, solvent-free synthesis, and utilization of silica-supported cataylst, which makes the overall methodology cost-effective, are the highlights of the methodology developed. The structures of the synthesized compounds were elucidated by spectral data. All spectral data were in accordance with assumed structures.

In vitro XO assay

All the synthetic compounds were evaluated for *in vitro* XO inhibitory activity. *In vitro* screening of the pyrimidones using bovine milk XO (grade 1, ammonium sulfate suspension) enzymatic assay was performed as described in the literature [16]. Allopurinol [17] was employed as reference inhibitors. The molecules exhibiting % age inhibition of more than 50% at 50 μM were further tested in triplicate for the XO inhibitory activity. The pyrimidones VA-2, VA-5, VA-7, VA-8, VA-9, VA-10, VA-12, VA-14, VA-15, VA-21, VA-22, VA-23, and VA-25 displayed percentage inhibition of more than 50% at 50 μM (Table 3) and were further considered for the calculation of IC_{50} values. The pyrimidones with heteroaryl ring (VA-12, VA-21, VA-22, VA-25) at position 4/6 or both displayed significant % inhibition of >80%. Among them, VA-12 and VA-25 possesing heteroaryl rings at both 4 and 6

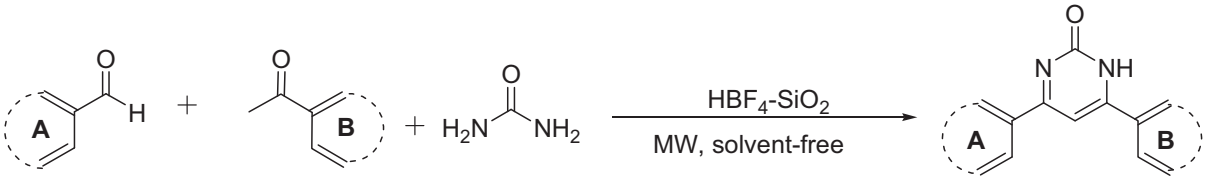

Scheme 1. Microwave-assisted synthesis of 4,6-diaryl/heteroarylpyrimidones.

Table 1. Percentage yields of the 4,6-diaryl/heteroarylpyrimidones with varying mol% of catalyst and time of exposure to microwave irradiation.

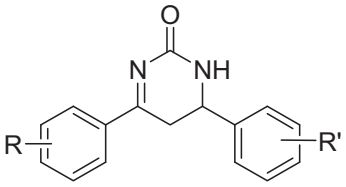

Entry	R	R′	Loading (mol%)	Time (MW)[a)]	Yield
1.	H	H	1	10	72
				15	67
				20	59
			5	10	82
				15	73
				20	68
			10	10	78
				15	70
				20	64
2.	4-Cl	H	1	10	79
				15	72
				20	68
			5	10	92
				15	84
				20	79
			10	10	87
				15	79
				20	73
3.	4-CH_3	H	1	10	76
				15	69
				20	63
			5	10	84
				15	76
				20	68
			10	10	77
				15	71
				20	63
4.	H	4-OCH_3	1	10	73
				15	67
				20	62
			5	10	85
				15	75
				20	69
			10	10	79
				15	71
				20	63
5.			1	10	56
				15	52
				20	47
			5	10	68
				15	62
				20	54
			10	10	61
				15	54
				20	50

[a)] Exposing the reaction mixture to microwave radiations for 5 min produced unsatisfactory yileds, i.e. <40%.

Table 2. Synthesized 4,6-substituted pyrimidones.

Code	Product	Yield (%)
VA-1	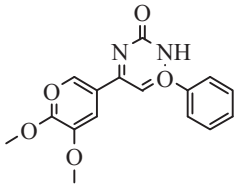	82
VA-2	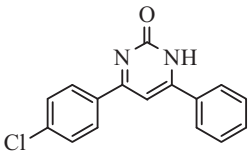	92
VA-3	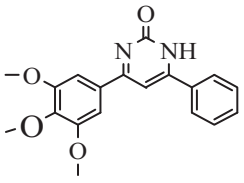	80
VA-4	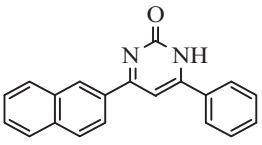	69
VA-5	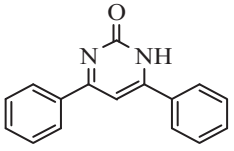	82
VA-6	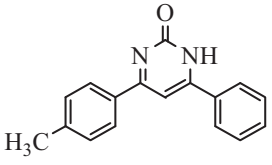	84
VA7	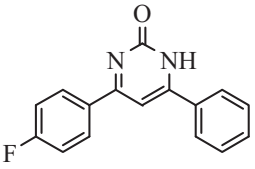	93
VA8	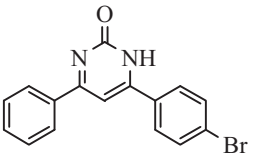	91
VA-9	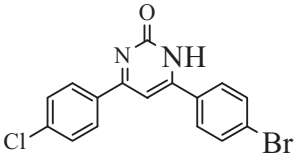	94

(*Continued*)

Table 2. (*Continued*)

Code	Product	Yield (%)
VA-10	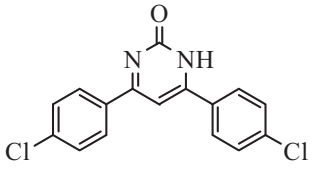	93
VA-11	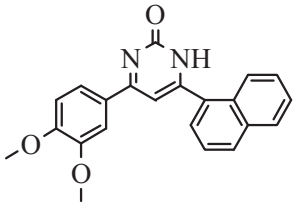	68
VA-12	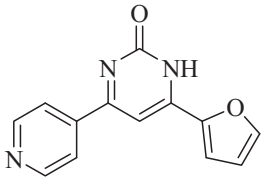	68
VA-13	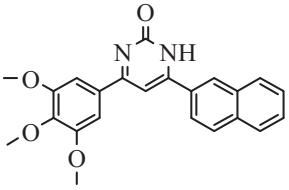	67
VA-14	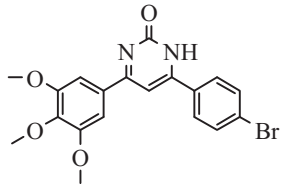	84
VA-15	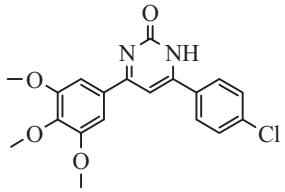	83
VA-16	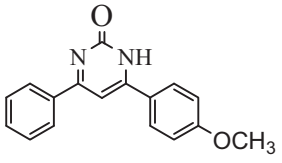	85
VA-17	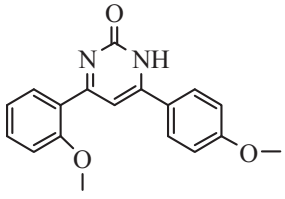	82

Table 2. (*Continued*)

Code	Product	Yield (%)
VA-18	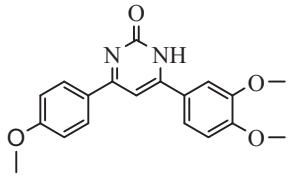	86
VA-19	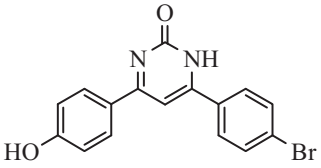	87
VA-20	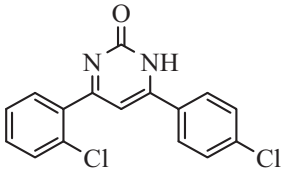	94
VA-21	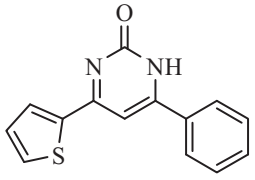	71
VA-22	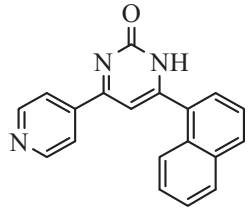	62
VA-23	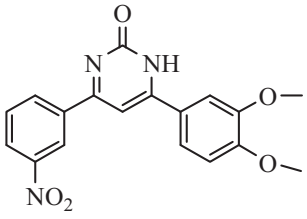	81
VA-24	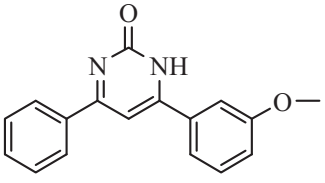	80
VA-25	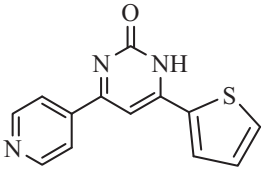	69

(*Continued*)

Table 3. *In vitro* screening of the synthesized compounds for XO inhibitory activity.

Compounds	Percentage inhibition (%)	IC_{50} (μM)[a)]
VA-1	40	–
VA-2	60	20.25
VA-3	39	–
VA-4	35.56	–
VA-5	90.32	10.21
VA-6	48	
VA-7	60.70	21.24
VA-8	79.50	15.67
VA-9	80.03	13.35
VA-10	76.26	12
VA-11	30.90	–
VA-12	95	7.23
VA-13	40.70	–
VA-14	69.13	18.87
VA-15	68.48	18.57
VA-16	45.11	–
VA-17	36.57	–
VA-18	25.90	–
VA-19	28.14	–
VA-21	81.85	13.46
VA-22	85.55	11.23
VA-23	68.90	18.93
VA-24	40.56	–
VA-25	97	6.45
Allopurinol		12.24

[a)] Values are mean of three experiments.

position were the most potent inhibitors with % inhibition of 95 and 97% (Table 3). This could be due to the hydrogen bonding ability of both the heteroatoms. Both VA-12 and -25 displayed low IC_{50} values of 7.23 and 6.45 μM as compared to allopurinol ($IC_{50} = 12.24$ μM). VA-25 with a pyridinyl ring as Ring A and thiophenyl as Ring B was the most potent inhibitor of the series. The slight difference in the inhibitory profile of VA-12 and VA-25 (both possesing a pyridinyl ring as Ring A) could be attributed to the higher aromatic character of 2-thiophenyl ring (Ring B) in VA-25 as compared to 2-furanyl ring (Ring B) in VA-12. Rings with higher aromatic character generally display stronger interactions with the amino acids posessing phenyl rings. This was further investigated by docking of VA-25 with in the active site of the enzyme.

Structure–activity relationship

From the data shown in Table 3, some generalizations about the structure–activity relationship were made such as: 1) Any substitutions on the phenyl rings (Ring A or Ring B or both) resulted in a decline in the inhibitory potential (compare V-5 with other pyrimidones except VA-12 and VA-25). 2) The decline in activity for the halo-substituted phenyl rings (at both 4th and 6th positions) was less as compared to other substituents. 3) Substitution of naphthyl ring either as Ring A and Ring B (VA-4, 11, 13) also displayed a decreased inhibitory profile. However, placement of heteroaryl ring (Ring A) and naphthyl ring (Ring B) in the chemical architecture of the designed pyrimidones regenerated the inhibitory potential (VA-22). 4) Placement of heteroaryl ring either on Ring A or Ring B proved to be extremely beneficial for the activity (VA-21, 22). 5) Placement of heteroaryl rings at both 4th and 6th positions (Ring A and Ring B) proved to be even more potent than compounds with monoheteroaryl ring. (Compare VA-12, VA-25 with VA-21, 22). On the basis of the results of *in vitro* XO inhibitors, a basic pharmacophore (Fig. 2) was formulated with the structural features required for XO inhibitory activity.

Molecular modeling studies

In order to theoretically investigate the recognition process of the most potent XO inhibitor VA-25, flexible docking experiment using GOLD software was performed assuming that it gets accommodated into the salicylic acid XO active site [18]. The docking study revealed some non-covalent interactions of the VA-25 at salicylic acid binding site of XO. The inhibitor VA-25 completely occupies the salicylic acid binding cavity of XO. In the binding conformation, VA-25 indicates some interaction, which may be crucial for the inhibition of XO. The thiophene ring in VA-25 is found to be involved in hydrogen bonding with side chain of Glu802. The π-electrons of thiophene ring also get engaged in face-to-face stacking with π-electrons of Phe914. This provides stability to the thiophene ring in the binding cavity. A strong hydrogen bonding was observed between the carbonyl group of VA-25 and hydroxyl group of the Ser876, which additionally help in stabilization of VA-25 in the binding cavity. The nitrogen of pyridine ring interacts with NH_2 group of Asn768. Thus, the docking result provides the rationale behind the XO inhibition (Fig. 3).

Calculation of molecular properties

The drug-like properties of the active compounds were calculated, which were found to be in accordance to Lipinski's rule of five (Table 4) [19]. The molecular properties of the most potent pyrimidones were found to be within the specified limits, which indicate their drug likeness.

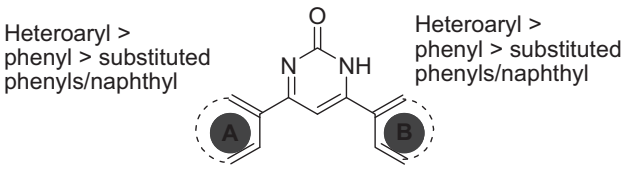

Figure 2. Pharmacophore.

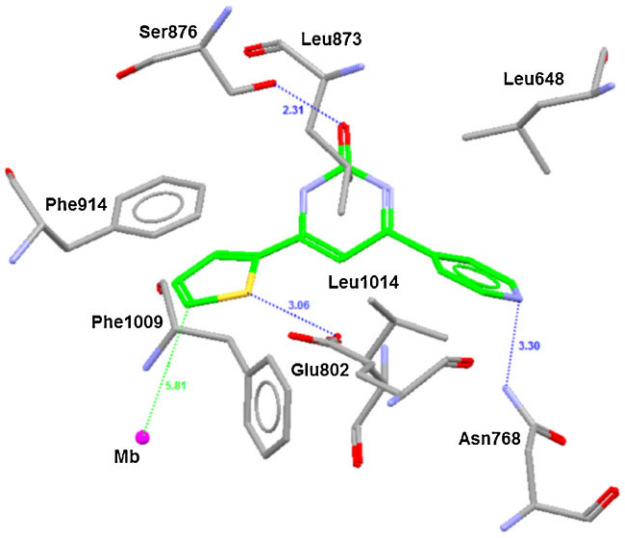

Figure 3. Binding mode of VA-25 at salicylic binding site of XO.

Conclusion

The present study provides an efficient methodology for the synthesis of 4,6-diarylpyrimidin-2(1*H*)-ones as a new class of XO inhibitors. HBF_4-SiO_2 at 5 mol% for 10 min under microwave conditions efficiently catalyzes all the reactions employing electronically and sterically diverse aldehydes/ketones. The synthesized compounds were evaluated for *in vitro* XO inhibitory potential. SAR study revealed that the nature of aryl ring and nature of substituent(s) on the aryl rings at positions 4 and 6 greatly affect the XO inhibitory activity. Pyrimidones with heteroaryl rings (both at 4th and 6th positions) as Ring A and Ring B were the most potent inhibitors. Docking simulations were performed to position most active compound VA-25 into the XO active site to determine the probable binding mode, and the results confirmed that the compound was a potential inhibitor of XO. Further detailed investigation will be carried out on VA-25, which appears to be a good hit among the series.

Experimental

The reagents were purchased from Sigma–Aldrich, Merck, CDH, Loba Chem., Spectro Chem., India and used without further purification. All yields refer to isolated products after purification. All the reactions were carried out in Biotage Microwave Synthesizer (Model: Initiator) operating at 150°C with the microwave power maximum level of 400 W. Products were characterized by comparison by spectroscopic data. ^{1}H NMR spectra were recorded on Bruker Advance II 400 NMR spectrometer and JEOL AL 300 NMR spectrometer. The spectra were measured in DMSO relative to TMS (0.00 ppm). Melting points were determined in open capillaries and were uncorrected.

Preparation of tetrafluoroboric acid adsorbed on silica gel (HBF_4-SiO_2)

The catalyst system HBF_4-SiO_2 was prepared following the originally reported method [20]. A mixture of silica gel (26.7 g, 300–400 mesh) and 40% aq. HBF_4 (3.3 g, 8.25 mL, 15 mmol) in diethyl ether (75 mL) was stirred for 3 h. The mixture was concentrated, and the residue dried under vacuum at 100°C for 72 h to afford HBF_4-SiO_2 (0.5 mmol HBF_4/g) as a free-flowing powder.

Procedure for the synthesis of 4,6-diaryl/heteroaryl-pyrimidin-2(1*H*)-one

To a 50 mL dried conical flask differently substituted benzaldehydes (1 mmol, 1 eq), acetophenones (5 mmol, 1 eq), urea (5 mmol, 1 eq), and 5 mol% of silicated flouroboric acid were added. The resulting mixture was placed into the microwave reactor for 10 min. On completion of the reaction, the crude mixture was dissolved in methanol and adsorbed on silica (60–120 #). The desired product was purified by column chromatography with increasing percentage of ethyl acetate in hexane as eluting solvent.

Characterization of synthesized compounds

4-(3,4-Dimethoxy-phenyl)-6-phenyl-1H-pyrimidin-2-one (VA-1)

Yellow powder; yield 78%; mp: 215–217°C; ^{1}H NMR ($CDCl_3$ + DMSO-d_6, 300 MHz, δ, TMS = 0): 8.04 (2H, *d*, J = 8.1 Hz), 7.54–7.85 (5H, *m*), 7.02 (1H, *d*, J = 7.5 Hz), 6.84 (1H, *d*, J = 7.2 Hz), 3.97 (3H, *s*, OCH_3), 3.93 (3H, *s*, OCH_3). Anal. calcd. for $C_{18}H_{16}N_2O_3$: C, 70.12; H, 5.23; N, 9.09. Found: C, 70.41; H, 5.04; N, 9.13.

4-(4-Chloro-phenyl)-6-phenyl-1H-pyrimidin-2-one (VA-2)

White powder; yield 78%; mp: 230–232°C; ^{1}H NMR (DMSO-d_6, 400 MHz, δ, TMS = 0): 8.23 (2H, *d*, J = 8 Hz), 8.16 (2H, *d*, J = 8 Hz), 7.48–7.65 (6H, *m*). Anal. calcd. for $C_{16}H_{11}ClN_2O$: C, 67.97; H, 3.92; N, 9.91. Found: C, 67.75; H, 4.03; N, 9.81.

6-Phenyl-4-(3,4,5-trimethoxy-phenyl)-1H-pyrimidin-2-one (VA-3)

Brown powder; yield 80%; mp: 249–251°C; ^{1}H NMR (DMSO-d_6, 400 MHz, δ, TMS = 0): 8.17 (2H, *bs*), 7.49–7.80 (4H, *m*), 7.45 (2H, *s*),

Table 4. Molecular properties of some potent compounds.

Entry	Compound	TPSA	Mol. wt.	ClogP	nOHNH	nON	nrotb
1	VA-12	71.78	239	1.29	1	5	2
2	VA-22	45.75	254	3.00	1	3	2
3	VA-23	58.68	299	3.14	1	4	2
4	VA-25	58.64	255	1.71	1	4	2

3.92 (6H, *s*, OCH_3), 3.78 (3H, *s*, OCH_3). Anal. calcd. for $C_{19}H_{18}N_2O_4$: C, 67.44; H, 5.36; N, 8.28. Found: C, 67.55; H, 5.12; N, 8.49.

4-Naphthalen-2-yl-6-phenyl-1H-pyrimidin-2-one (VA-4)

Brown powder; yield 81%; mp: 267–269°C; ^{1}H NMR (DMSO-d_6, 400 MHz, δ, TMS = 0): 11.25 (1H, *s*, NH, D_2O exchangeable proton), 8.10–8.20 (4H, *m*), 7.77–7.78 (1H, *d*, $J = 8$ Hz), 7.58–7.78 (8H, *m*). Anal. calcd. for $C_{20}H_{14}N_2O$: C, 80.52; H, 4.73; N, 9.39. Found: C, 80.33; H, 4.92; N, 9.21.

4,6-Diphenyl-1H-pyrimidin-2-one (VA-5)

Yellow powder; yield 89%; mp: 270–272°C; ^{1}H NMR (DMSO-d_6, 300 MHz, δ, TMS = 0): 11.13 (1H, *s*, NH, D_2O exchangeable protons), 8.15–8.16 (4H, *m*), 7.54–7.56 (7H, *m*). Anal. calcd. for $C_{16}H_{12}N_2O$: C, 77.40; H, 4.87; N, 11.28. Found: C, 77.35; H, 4.98; N, 11.03.

6-Phenyl-4-p-tolyl-1H-pyrimidin-2-one (VA-6)

White powder; yield 79%; mp: 255–257°C; ^{1}H NMR (DMSO-d_6, 400 MHz, δ, TMS = 0): 11.32 (1H, *s*, NH, D_2O exchangeable protons), 8.16 (2H, *d*, $J = 8$ HZ), 8.08 (2H, *d*, $J = 8$ Hz), 7.53–7.61 (4H, *m*), 7.37 (2H, *d*, $J = 8$ Hz), 2.49 (3H, *s*, CH_3). Anal. calcd. for $C_{17}H_{14}N_2O$: C, 77.84; H, 5.38; N, 10.68. Found: C, 78.01; H, 5.41; N, 10.55.

4-(4-Fluoro-phenyl)-6-phenyl-1H-pyrimidin-2-one (VA-7)

Light yellow powder; yield-90%; mp: 265–267°C; ^{1}H NMR (DMSO-d_6, 400 MHz, δ, TMS = 0): 11.20 (1H, *s*, NH, D_2O exchangeable protons), 8.29 (2H, *d*, $J = 8$ Hz), 8.16 (2H, *d*, $J = 8$ Hz), 7.56–7.71 (3H, *m*), 7.39–7.47 (3H, *m*). Anal. calcd. for $C_{16}H_{11}FN_2O$: C, 71.17; H, 4.16; N, 10.52. Found: C, 71.99; H, 3.89; N, 10.64.

6-(4-Bromo-phenyl)-4-phenyl-1H-pyrimidin-2-one (VA-8)

White powder; yield 70%; mp: 279–280°C; ^{1}H NMR (DMSO-d_6, 300 MHz, δ, TMS = 0): 8.04 (4H, *m*), 7.66 (2H, *d*, $J = 7.2$ Hz), 7.52–7.55 (4H, *m*). Anal. calcd. for $C_{16}H_{11}BrN_2O$: C, 58.74; H, 3.39; N, 8.56. Found: C, 58.82; H, 3.49; N, 8.42.

6-(4-Bromo-phenyl)-4-(4-chloro-phenyl)-1H-pyrimidin-2-one (VA-9)

Yellow powder; yield 85%; mp: 278–280°C; ^{1}H NMR (DMSO-d_6, 400 MHz, δ, TMS = 0): 8.22 (2H, *d*, $J = 8$ Hz, Ar-H), 8.16 (2H, *d*, $J = 8.00$ Hz), 7.78 (2H, *d*, $J = 8$ Hz), 7.68 (1H, *m*), 7.64 (2H, *d*, $J = 8$ Hz). Anal. calcd. for $C_{16}H_{10}BrClN_2O$: C, 53.14; H, 2.79; N, 7.75. Found: C, 52.93; H, 3.03; N, 8.02.

4,6-Bis-(4-chloro-phenyl)-1H-pyrimidin-2-one (VA-10)

Yellow powder; yield 88%; mp: 274–276°C; ^{1}H NMR (DMSO-d_6, 400 MHz, δ, TMS = 0): 12.12 (1H, *s*, NH, D_2O exchangeable protons), 8.24 (4H, *bs*), 7.63–7.65 (5H, *m*). Anal. calcd. for $C_{16}H_{10}Cl_2N_2O$: C, 60.59; H, 3.18; N, 8.83. Found: C, 60.83; H, 2.88; N, 9.10.

4-(3,4-Dimethoxy-phenyl)-6-naphthalen-2-yl-1H-pyrimidin-2-one (VA-11)

Dark yallow powder; yield 76%; mp: 279–281°C; ^{1}H NMR (DMSO-d_6, 400 MHz, δ, TMS = 0): 11.17 (1H, *s*, NH, D_2O exchangeable protons), 8.11 (1H, *d*, $J = 8$ Hz), 8.04 (1H, *d*, $J = 8$ Hz), 7.22–7.61 (6H, *m*), 7.06–7.18 (3H, *m*), 3.86 (6H, *s*, OCH_3). Anal. calcd. for $C_{22}H_{18}N_2O_3$: C, 73.73; H, 5.06; N, 7.82. Found: C, 74.00; H, 4.77; N, 8.18.

6-Furan-2-yl-4-pyridin-4-yl-1H-pyrimidin-2-one (VA-12)

Light brown powder, yield 89%; mp: 272–274°C; ^{1}H NMR ($CDCl_3$ +DMSO-d_6, 300 MHz, δ, TMS = 0): 8.45–8.76 (3H, *m*), 7.66 (2H, *d*, $J = 4.8$ Hz), 7.21–7.40 (3H, *m*). Anal. calcd. for $C_{13}H_9N_3O_2$: C, 65.27; H, 3.79; N, 17.56. Found: C, 65.38; H, 3.54; N, 17.69.

6-Naphthalen-2-yl-4-(3,4,5-trimethoxy-phenyl)-1H-pyrimidin-2-one (VA-13)

Yellow powder; yield 81%; mp: 267–269°C; ^{1}H NMR (DMSO-d_6, 400 MHz, δ, TMS = 0): 8.82(1H, *bs*), 8.29 (1H, *bs*), 8.02–8.12 (3H, *m*), 7.30–7.61 (5H, *m*), 3.94 (6H, *s*, OCH_3), 3.77 (3H, *s*, OCH_3). Anal. calcd. for $C_{23}H_{20}N_2O_4$: C, 71.12; H, 5.19; N, 7.21. Found: C, 70.95; H, 4.91; N, 7.38.

6-(4-Bromo-phenyl)-4-(3,4,5-trimethoxy-phenyl)-1H-pyrimidin-2-one (VA-14)

White powder; yield 79%; mp: 278–280°C; ^{1}H NMR (DMSO-d_6, 400 MHz, δ, TMS = 0): 8.16 (2H, *d*, $J = 8$ Hz), 7.77–7.79 (3H, *m*), 7.44 (2H, *d*, $J = 8$ Hz), 3.92 (6H, *s*, OCH_3), 3.75 (3H, *s*, OCH_3). Anal. calcd. for $C_{19}H_{17}BrN_2O_4$: C, 54.69; H, 4.11; N, 6.71. Found: C, 54.97; H, 3.88; N, 6.94.

6-(4-Chloro-phenyl)-4-(3,4,5-trimethoxy-phenyl)-1H-pyrimidin-2-one (VA-15)

Yellow powder; yield 85%; mp: 266–267°C; ^{1}H NMR (DMSO-d_6, 400 MHz, δ, TMS = 0): 8.25 (2H, *d*, $J = 8$ Hz), 7.64–7.71 (3H, *m*), 7.45 (2H, *d*, $J = 8$ Hz), 3.92 (6H, *s*, OCH_3), 3.75 (3H, *s*, OCH_3). Anal. calcd. for $C_{19}H_{17}ClN_2O_4$: C, 61.21; H, 4.60; N, 7.51. Found: C, 61.38; H, 4.76; N, 7.32.

6-(4-Methoxy-phenyl)-4-phenyl-1H-pyrimidin-2-one (VA-16)

White powder; yield 80%; mp: 237–239°C; ^{1}H NMR (DMSO-d_6, 400 MHz, δ, TMS = 0): 11.20 (1H, *s*, NH, D_2O exchangeable protons), 8.09–8.15 (4H, *m*), 7.53–7.61 (3H, *m*), 7.44 (1H, *s*), 7.09–7.10 (2H, *d*, $J = 8.00$ Hz), 3.84 (3H, *s*, OCH_3). Anal. calcd. for $C_{17}H_{14}N_2O_2$: C, 73.37; H, 5.07; N, 10.07. Found: C, 73.22; H, 4.76; N, 9.86.

6-(4-Methoxy-phenyl)-4-(2-methoxy-phenyl)-1H-pyrimidin-2-one (VA-17)

Brown powder; yield 90%; mp: 240–242°C; ^{1}H NMR (DMSO-d_6, 400 MHz, δ, TMS = 0): 8.11 (2H, *bs*), 7.21–7.71 (4H, *m*), 7.15 (1H, *m*), 7.09 (2H, *d*, $J = 8$Hz), 3.81 (6H, *s*, OCH_3). Anal. calcd. for $C_{18}H_{16}N_2O_3$: C, 70.12; H, 5.23; N, 9.09. Found: C, 69.84; H, 5.46; N, 8.78.

6-(3,4-Dimethoxy-phenyl)-4-(4-methoxy-phenyl)-1H-pyrimidin-2-one (VA-18)

Yellow powder, yield 90%; mp: 255–257°C; ^{1}H NMR (DMSO-d_6, 400 MHz, δ, TMS = 0): 8.16 (2H, *d*, $J = 6$ Hz), 7.80 (1H, *bs*), 7.70 (1H, *bs*), 7.42 (1H, *s*), 7.09–7.12 (3H, *m*), 3.89 (3H, *s*, OCH_3), 3.86 (6H, *s*, OCH_3). Anal. calcd. for $C_{19}H_{18}N_2O_4$: C, 67.44; H, 5.36; N, 8.28. Found: C, 67.66; H, 5.42; N, 8.19.

6-(4-Bromo-phenyl)-4-(4-hydroxy-phenyl)-1H-pyrimidin-2-one (VA-19)

Yellow powder; yield 78%; mp: 239–241°C; ^{1}H NMR (DMSO-d_6, 300 MHz, δ, TMS = 0): 8.00 (2H, *d*, *J* = 8Hz), 7.89–7.93 (3H, *m*), 7.64 (2H, *d*, *J* = 7.5Hz), 6.92 (2H, *d*, *J* = 7.5 Hz). Anal. calcd. for $C_{16}H_{11}BrN_2O_2$: C, 56.00; H, 3.23; N, 8.16. Found: C, 56.38; H, 3.11; N, 7.95.

6-(4-Chloro-phenyl)-4-(2-chloro-phenyl)-1H-pyrimidin-2-one (VA-20)

Yellow powder; yield 84%; mp: 274–276°C; ^{1}H NMR (DMSO-d_6, 400 MHz, δ, TMS = 0): 11.17 (1H, *s*, NH, D_2O exchangeable proton), 8.18 (3H, *m*), 7.71–7.72 (6H, *m*). Anal. calcd. for $C_{16}H_{10}Cl_2N_2O$: C, 60.59; H, 3.18; N, 8.83. Found: C, 60.73; H, 2.81; N, 9.09.

6-Phenyl-4-thiophen-2-yl-1H-pyrimidin-2-one (VA-21)

Brown powder; yield 87%; mp: 277–279°C; ^{1}H NMR (DMSO-d_6, 400 MHz, δ, TMS = 0): 11.21 (1H, *s*, NH, D_2O exchangeable proton), 8.23 (1H, *d*, *J* = 4 Hz), 8.03–8.00 (2H, *m*), 7.88 (1H, *d*, *J* = 4 Hz), 7.56–7.61 (4H, *m*), 7.28 (1H, *m*). Anal. calcd. for $C_{14}H_{10}N_2OS$: C, 66.12; H, 3.96; N, 11.02; S, 12.61 Found: C, 66.12; H, 3.96; N, 11.02; S, 12.61.

6-Naphthalen-1-yl-4-pyridin-4-yl-1H-pyrimidin-2-one (VA-22)

Brown powder; yield 80%; mp: 239–241°C; ^{1}H NMR (DMSO-d_6, 400 MHz, δ, TMS = 0): 11.19 (1H, *s*, NH, D_2O exchangeable proton), 8.20–8.35 (4H, *m*), 7.50–7.62 (8H, *m*). Anal. calcd. for $C_{19}H_{13}N_3O$: C, 76.24; H, 4.38; N, 14.04. Found: C, 76.05; H, 4.62; N, 13.89.

6-(3,4-Dimethoxy-phenyl)-4-(3-nitro-phenyl)-1H-pyrimidin-2-one (VA-23)

Yellow powder; yield 89%; mp: 248–250°C; ^{1}H NMR (DMSO-d_6, 400 MHz, δ, TMS = 0): 8.69 (1H, *s*), 8.43 (1H, *d*, *J* = 8 Hz), 7.75–7.89 (5H, *m*), 7.14 (1H, *d*, *J* = 8 Hz), 3.90 (3H, *s*, OCH_3), 3.85 (3H, *s*, OCH_3). Anal. calcd. for $C_{18}H_{15}N_3O_5$: C, 61.19; H, 4.28; N, 11.89. Found: C, 60.82; H, 4.17; N, 12.15.

6-(3-Methoxy-phenyl)-4-phenyl-1H-pyrimidin-2-one (VA-24)

Yellow powder; yield 90%; mp: 237–240°C; ^{1}H NMR (DMSO-d_6, 300 MHz, δ, TMS = 0): 11.17 (1H, *s*, NH, D_2O exchangeable proton), 8.18 (2H, *d*, *J* = 8 Hz), 7.28–7.71 (7H, *m*), 7.15 (1H, *d*, *J* = 8 Hz), 3.83 (3H, *s*, OCH_3). Anal. calcd. for $C_{17}H_{14}N_2O_2$: C, 73.37; H, 5.07; N, 10.07. Found: C, 73.47; H, 4.94; N, 9.88.

4-(Pyridin-4-yl)-6-(thiophen-2-yl)pyrimidin-2(1H)-one (VA-25)

Light brown powder; yield 88%; mp: 275–276°C; ^{1}H NMR (DMSO-d_6, 300 MHz, δ, TMS = 0): 8.73 (2H, *d*, J = 4 Hz), 8.19 (1H, *d*, *J* = 4 Hz), 8.00 (2H, *bs*), 7.83 (2H, *m*), 7.23 (1H, *dd*, *J* = 2 and 4 Hz); Anal. calcd. for $C_{13}H_9N_3OS$: C, 61.16; H, 3.55; N, 16.46; S, 12.56 Found: C, 60.97; H, 3.66; N, 16.09; S, 12.44.

Xanthine oxidase assay

Bovine milk XO (grade 1, ammonium sulfate suspension; Sigma–Aldrich) activity was assayed spectrophotometrically by measuring the uric acid formation at 293 nm [16b, 21] using a Bluestar AU-2701 UV–Visible spectrophotometer at 25°C. The reaction mixture contained 50 mM potassium phosphate buffer (pH 7.6), 75 mM xanthine, and 0.08 units of XO. Inhibition of XO activity by various inhibitors was measured by following the decrease in the uric acid formation at 293 nm at 25°C. The enzyme was preincubated for 5 min with the test compound dissolved in DMSO (1% v/v), and the reaction was started by the addition of xanthine. Final concentration of DMSO (1% v/v) did not interfere with the enzyme activity. All the experiments were performed in triplicate and values were expressed as means of three experiments.

Molecular modeling

A flexible docking study of most active compound at the salicylic acid binding site of XO was performed with the help of GOLD software [22]. To validate the docking procedure for the prediction of the correct binding mode of inhibitor at the salicylic acid binding site, salicylic acid was extracted from the original X-ray structure (1FIQ) [18] and re-docked. The highest scoring conformation was selected and compared with X-ray structure conformation. The docked conformation of salicylic acid was found to be similar to the original X-ray structure. The root mean square deviation between the best scored conformers from docking and X-ray structure was found to be 0.21 Å.

The authors are grateful to the vice chancellor Dr. A. S. Brar and Dr. Palwinder Singh, Associate Professor, Department of Chemistry, Guru Nanak Dev University, Amritsar for providing the facilities necessary for the present study.

The authors have declared no conflict of interest.

References

[1] A. L. Stockert, S. S. Shinde, R. F. Anderson, R. Hille, *J. Am. Chem. Soc.* **2002**, *124*, 14554–14555.

[2] F. Borges, E. Fernandes, F. Roleira, *Curr. Med. Chem.* **2002**, *9*, 195–217.

[3] H. Hille, *Eur. J. Inorg. Chem.* **2006**, 1913–1926.

[4] (a) R. Dhiman, S. Sharma, G. Singh, K. Nepali, P. M. S. Bedi, *Arch. Pharm.* **2013**, *346* (1), 7–16. (b) G. B. Elion, S. Callahan, H. Nathan, S. Bieber, R. W. Rundles, G. H. Hitching, *Biochem. Pharmacol.* **1963**, *12*, 85–93. (c) H. Tamta, R. Thilagavathi, A. K. Chakraborti, A. K. Mukhopadhyay, *J. Enzyme Inhib. Med. Chem.* **2005**, *20*, 317–324.

[5] P. Pacher, A. Nivorozhkin, *C. Szabó Pharmacol. Rev.* **2006**, *58*, 87–114.

[6] R. K. Robins, G. R. Revankar, D. E. Brien, R. H. Springer, T. N. A. Albert, K. Senga, J. P. Miller, D. G. J. Streeter, *J. Heterocycl. Chem.* **1985**, *22*, 601–634.

[7] K. Oettl, G. Reibneggar, *Biochim. Biophys. Acta.* **1999**, *1430*, 387–395.

[8] K. Nepali, G. Singh, A. Turan, A. Agarwal, S. Sapra, R. Kumar, U. C. Banerjee, P. K. Verma, N. K. Satti, M. K. Gupta, O. P. Suri, K. L. Dhar, *Bioorg. Med. Chem.* **2011**, *19*, 1950–1958.

[9] K. Nepali, A. Agarwal, S. Sapra, V. Mittal, R. Kumar, U. C. Banerjee, M. K. Gupta, N. K. Satti, O. P. Suri, K. L. Dhar, *Bioorg. Med. Chem.* **2011**, *19*, 5569–5576.

[10] S. Sharma, K. Sharma, R. Ojha, D. Kumar, G. Singh, K. Nepali, P. M. S. Bedi, *Bioorg. Med. Chem. Lett.* **2014**, *24* (2), 495–500.

[11] S. S. Sandhu, J. S. Sandhu, *ARKIVOC* **2012**, (i) 66–133.

[12] (a) M. R. Ahmad, V. G. Sastry, Y. R. Prasad, M. H. R. Khan, N. Bano, S. Anwar, *Eur. J. Chem.* **2012**, *3* (1), 94–98. (b) Y. Dai, M. Cao, M. Zhuang, S. Xia, S. Tu, L. Rong, *Syn. Commun.* **2011**, *41*, 3039–3044. (c) M. M. Heravi, L. Ranjbar, F. Derikvand, B. Alimadad, *Mol. Divers.* **2008**, *12*, 191–196; (d) S. R. Mistry, K. C. Maheria, *J. Mol. Catal. A Chem.* **2012**, *355*, 210–215.

[13] (a) S. Rudrawar, R. C. Besra, A. K. Chakraborti, *Synthesis* **2006**, *16*, 2767–2771. (b) A. K. Chakraborti, S. V. Chankeshwara, *Org. Biomol. Chem.* **2006**, *4*, 2769–2771. (c) A. K. Chakraborti, R. Gulhane, *Tetrahedron Lett.* **2003**, *44*, 3521–3525. (d) A. K. Chakraborti, R. J. Gulhane, *Chem. Soc. Chem. Commun.* **2003**, 1896–1897; (e) G. Sharma, R. Kumar, A. K. Chakraborti, *Tetrahedron Lett.* **2008**, *49*, 4272–4275. (f) D. Kumar, R. Kumar, A. K. Chakraborti, *Synthesis* **2008**, *8*, 1249–1256. (g) R. Kumar, D. Kumar, A. K. Chakraborti, *Synthesis* **2007**, *2*, 299–303.

[14] B. P. Bandgar, S. S. Gawande, S. C. Warangkar, *Bioorg. Med. Chem. Lett.* **2010**, *18*, 3618–3624.

[15] (a) S. H. Mashraqui, M. B. Patil, H. D. Mistry, S. Ghadigaonkar, A. Meetsmay, *Chem. Lett.* **2004**, *33*, 1058–1059; (b) J. Yu, F. Shi, L. Z. Gong, *Acc. Chem. Res.* **2011**, *44* (11), 1156–1171. (c) G. Brahmachari, D. Suvankar, *Tetrahedron Lett.* **2012**, *53*, 1479–1482. (d) G. C. Nandi, S. Samai, R. Kumar, M. S. Singh, *Tetrahedron Lett.* **2009**, *50*, 7220–7222.

[16] (a) J. Escribano, F. Gracia-Canovas, *Biochem. J.* **1988**, *254*, 829–833; (b) Y. Takano, K. Hase-Aoki, H. Horiuchi, L. Zhao, Y. Kasahara, S. Kondo, M. A. Becker, *Life Sci.* **2005**, *76*, 1835–1847.

[17] P. Pacher, A. Nivorozhkin, C. Szabó, *Pharmacol. Rev.* **2006**, *58*, 87–114.

[18] C. Enroth, B. T. Eger, K. Okamoto, T. Nishino, E. F. Pai, *Proc. Natl. Acad. Sci.* **2000**, *97*, 10723–10728.

[19] Calculated from http://www.molinspiration.com/cgi-bin/properties

[20] A. K. Chakraborti, R. Gulhane, *Tetrahedron Lett.* **2003**, *44*, 3521–3525.

[21] J. Escribano, F. Gracia-Canovas, *Biochem. J.* **1988**, *254*, 829–833.

[22] GOLD, Evaluation Version 4.0.1. Cambridge Crystallographic Data Centre, Cambridge, UK **2009**.

